https://doi.org/10.5194/tc-2021-352
Preprint. Discussion started: 21 December 2021

The Cryosphere Discussions
Open Access
EGU

Modelling Glacier Evolution in Bhutanese Himalaya during the Little Ice Age

Weilin Yang[1], Yingkui Li[2], Gengnian. Liu[1], Wenchao Chu[3]

[1]College of Urban and Environmental Sciences, Peking University, Beijing 100871, China.
[2]Department of Geography, University of Tennessee, Knoxville, TN 37996, USA.
[3]Department of Earth System Science, Ministry of Education Key Laboratory for Earth System Modeling, Institute for Global Change Studies, Tsinghua University, Beijing 100084, China.

Correspondence to: Wenchao Chu (peterchuwenchao@foxmail.com)

Abstract. Mountain glaciers provide as a window into past climate change and landscape evolution, but the pattern of glacier evolution at centennial or suborbital timescale remains elusive, especially in monsoonal Himalayas. We simulated the glacier evolution in Bhutanese Himalaya, a typical monsoon influenced region, during the Little Ice Age (LIA), using the Open Global Glacier Model and six paleo-climate datasets. Compared with the mapped glacial landforms, the model can well capture the glacier length changes, especially for the experiment driving by the GISS climate dataset, but overestimates the changes in glacier area. Simulation results reveal four glacial substages at 1270s-1400s, 1470s-1520s, 1700s-1710s, and 1820s-1900s in the study area. From further analysis, a negative correlation between the number of the substages and glacier length was found, which suggests that the number and occurrence of glacial substages are regulated by the heterogeneous responses of glaciers to climate change. In addition, the changes in summer temperature dominated the glacier evolution in this region during the LIA.

1 Introduction

Mountain glaciers over high Himalayas provide as a critical window to explore the linkage between climatic, tectonic, and glacial systems (Oerlemans et al., 1998; Owen et al., 2009; Dortch et al., 2013; Owen & Dortch, 2014; Saha et al., 2018). Many scientists have investigated the glacial history for Himalayas at orbital-scale, indicating that a general trend of glacier advances is related to overall summer temperature, forced by orbitally-controlled insolation (Murari et al., 2014; Yan et al., 2018, 2020, 2021). However, latest observations with finer temporal resolution have revealed that the evolution of some glaciers in monsoonal Himalayas has suborbital-scale fluctuations, which has aroused more and more interest on exploring the mechanisms behind (Solomina et al., 2015; Peng et al., 2020).

The Little Ice Age (LIA; from 1300 to 1850 CE; Grove, 2013; Qureshi et al., 2021) is the latest cooling event during the Holocene, during which most mountain glaciers advanced, forming abundant well-preserved and distinctive geomorphic landforms (Murari et al., 2014; Qiao & Yi, 2017; Peng et al., 2019, 2020). Previous studies have reconstructed the timing and extent of glacier evolution during the LIA based on field investigation, geomorphological mapping, and cosmogenic nuclide

https://doi.org/10.5194/tc-2021-352
Preprint. Discussion started: 21 December 2021

dating (Owen & Dortch, 2014 and references therein; Zhang et al., 2018a, 2018b; Carrivick et al., 2019; Qureshi et al., 2021). However, dating glacial landform is challenging due to the post glacial degradation and the large uncertainties in the dating methods (Heyman et al., 2011; Fu et al., 2013). In addition, the reconstructions using individual glaciers or a small number of glaciers may be not representative for the regional average (Carrivick et al., 2019). It is therefore still unclear on how many substages exist during the LIA and how to separate the contribution of precipitation and temperature on glacier evolution.

Numerical glacial modelling is a powerful way to study glacier evolution on centennial timescale (Parkes & Goosse, 2020) and quantify the response of glaciers to climate change (Eis et al., 2019). The modelling approach can largely alleviate the limitations of field-based methods in exploring response of glaciers to climate change on the regional scale and provides an opportunity to understand the pattern of glacier change during the LIA. The model simulation can be cross validated using multiple observational records. However, evaluating the simulation results is still challenging due to the scarcity of the direct observational record for glacier changes during the LIA (Goosse et al., 2018).

The ongoing debate about the pattern of glacier evolution during the LIA is, in part, resulted from an imperfect understanding on how to cross validate observation with simulation, what the contribution of individual glacier to regional glacier evolution is, and how climate change drives glacier evolution (Goosse et al., 2018; Carrivick et al., 2019; Peng et al., 2019, 2020). Based on previous works, this study improves the understanding of the pattern of LIA glacier changes in Bhutanese Himalaya (BH; Fig. 1), a typical monsoon-influenced area, using the Open Global Glacier Model (OGGM). We systematically simulated the glacier changes during the LIA based on the climate data from six different general circulation models (GCMs). The simulated changes in glacier length, area and equilibrium line altitude (ELA) are validated by geomorphological maps and previous studies. The pattern of regional glacial evolution is compared with ^{10}Be glacial chronologies across the monsoon influenced Himalayas. The dominant climatic factors of the regional glacial evolution are explored through a series of sensitivity experiments.

https://doi.org/10.5194/tc-2021-352
Preprint. Discussion started: 21 December 2021

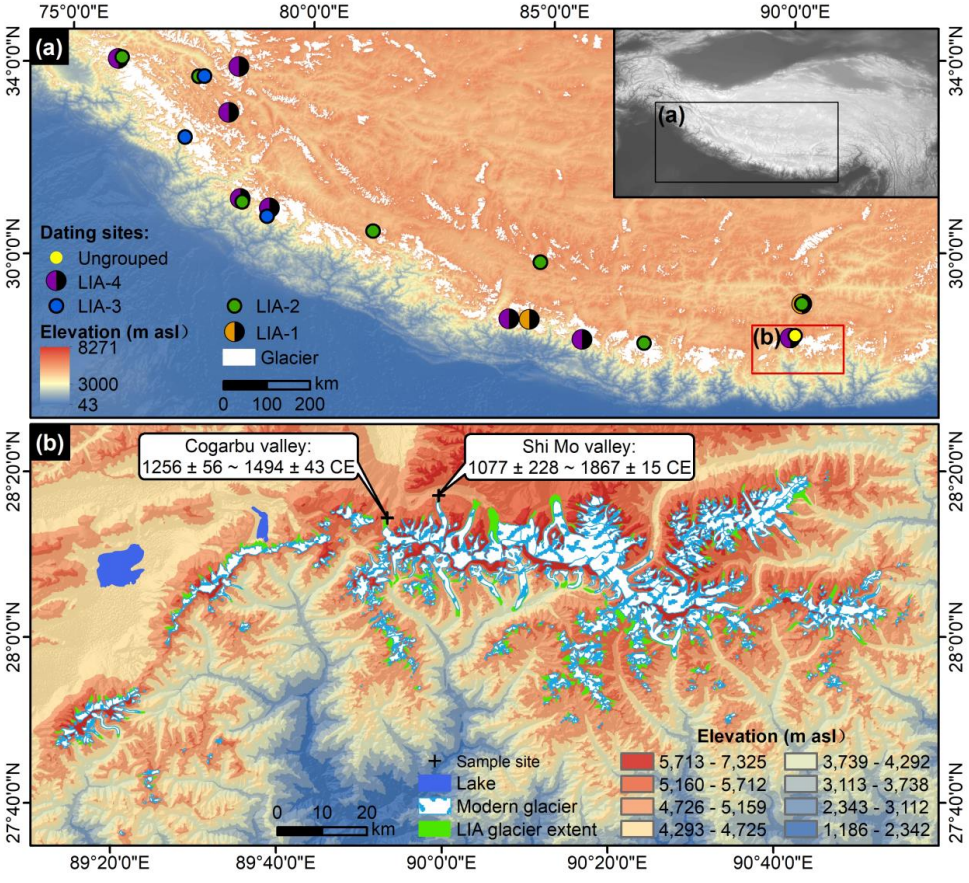

Figure 1. (a) The distribution of the ^{10}Be surface exposure dating sites in monsoonal Himalayas. The ^{10}Be surface exposure ages are recalculated using CRONUS Earth V3 online calculator (Balco et al., 2008; http://hess.ess.washington.edu/math/) and the moraine ages are determined based on the criterion in Peng et al. (2019) (see Text S1, Table S1 and Fig. S1 for details). (b) Mapped 408 glaciers during the LIA and the contemporary periods. The ages of the LIA moraines in BH are from Peng et al. (2019, 2020).

2 Methods

2.1 The Open Global Glacier Model

The OGGM is a 2D ice-flow model, to simulate past and future mass-balance, volume, and geometry of glaciers (Maussion et al., 2019). Studies indicated that a good performance of this model in simulating alpine glaciers (Farinotti et al., 2017; Pelto et al., 2020) and reproducing the millennial trend of glacial evolution in mountainous regions (Goosse et al., 2018; Parkes & Goosse, 2020).

The OGGM couples a surface mass balance (SMB) scheme with a dynamic core. The dynamic core is based on the shallow-ice approximation (SIA), computing the depth-integrated ice flux of each cross-section along multiple connected flowlines that are diagnosed from a pre-process algorithm. The spatial resolution (dx; m) of the target grid is scale dependent, determined by the size of the glacier ($dx=14S^{\frac{1}{2}}+10$, with S representing the glacier area in km^2) and a predefined minimum (10

https://doi.org/10.5194/tc-2021-352
Preprint. Discussion started: 21 December 2021


The Cryosphere Discussions

m) and maximum (200 m) values, respectively (Bahr et al., 2014). The ice accumulation is estimated by a solid precipitation scheme to separate the total precipitation into rain and snow based on monthly air temperature. In this scheme, the amount of solid precipitation is computed as a fraction of the total precipitation. Specially, precipitation is entirely solid if $T_i <= T_{Solid}$ (default setting is 0 ℃), entirely liquid if $T_i >= T_{Liquid}$ (defaults to 2 ℃) or divided into solid and liquid parts based on a linear relationship with those two temperature values. The ablation is estimated using a positive degree-day (PDD) scheme (Eq. 1). Melting occurs if monthly temperature ($T_i(z)$) is above T_{melt}, which is equal to -1 ℃.

$$m_i(z)=p_f P_i^{solid}(z)-\mu^* \cdot max(T_i(z)+\beta-T_{melt},0)+\varepsilon, \quad (1)$$

where $m_i(z)$ is the monthly SMB at elevation z of month i. $P_i^{solid}(z)$ is the monthly solid precipitation, and P_f is a general precipitation correction factor (default setting is 2.5). β is the temperature bias (defaults to 0 ℃) and a residual bias term (ε) is added as a tuning parameter to represent the collective effects of non-climate factors. Different from the conventional PDD schemes embedded in other ice sheet models, such as Parallel Ice Sheet Model (Bueler & Brown, 2009; Winkelmann et al., 2011), SICOPOLIS (Greve, 1997a, 1997b) or CISM (Lipscomb et al., 2019), that assume ε and μ^* as constant values, these parameters vary with glacier in OGGM to better capture the changes of individual glaciers.

2.2 Climate forcing and experimental design

The temperature and precipitation datasets from six different GCMs (BCC-CSM, CCSM4, CESM, GISS, IPSL, MPI) were used as climate forcing to drive OGGM. These data are available in the Past Model Intercomparison Project (PMIP3) and the Coupled Model Intercomparison Project (CMIP5) protocols (Schmidt et al., 2011; Tayloret al., 2012; PAGES 2k-PMIP3 group, 2015) – with details listed in Goosse et al. (2018) and Table S2. The climate data cannot be directly used in glacial model due to the systematical bias in the climate datasets produced by different GCMs. A calibration algorithm is adopted by OGGM to correct the GCMs climate data series by taking the anomalies between GCMs and the CRU TS 4.01 mean climate from 1961 to 1990 (Parkes et al., 2020).

To better estimate the long-term glacier evolution for each GCM forcing, the spin-up procedures and parameter tunning are required to initiate the model, because the model is sensitive to the initial condition (Eis et al., 2019). A 600-year spin-up is conducted using annual climate data selected randomly from a 51-year window of 875-925 CE from the corresponding GCM prior to the long-term integrations. The tunable parameter, β, in Equation S1 is set as -1℃ based on a set of sensitivity tests in which we adjust β from -1 to 1 ℃ with an increment of 1 ℃. We found that simulation results of the first ~250 years are sensitive to β that larger β will lead to smaller glacier initial state, but such sensitivity rapidly diminishes in the long-term simulation. Thus, the only criterion for we to tune β is to ensure the LIA start time close to the ^{10}Be chronologies in BH. After spin-up, the simulations are conducted during the period of 900-2000 CE for all glacial evolution experiments. Because the simulation of the first 100 years (900-1000 CE) is influenced by the choice of initial conditions, we limit our analyses to the

https://doi.org/10.5194/tc-2021-352
Preprint. Discussion started: 21 December 2021

simulations in 1000-2000 CE to examine the glacier response to climate trends (Goosse et al., 2018; Parkes, et al., 2020).

We also test the sensitivity of glaciers to temperature and precipitation through control experiments. We apply a 'constant climate scenario', use the CRU datasets as the climate forcing, and run the simulation until reaching equilibrium (piControl). The window size is set to 51-year and centered on t^*, the year for which the surface mass balance (SMB) scheme best reproduces the observed SMB. We set ε to 0 in Eq. 1, in order to maintain the contemporary glacier geometry under the contemporary climate condition. Then, keeping the same precipitation, stepwise changes (at 0.1 ℃) in annual temperature from -1 to 1 ℃ are uniformly added to the CRU datasets to test the sensitivity of temperature on glacier evolution. The similar analysis is conducted to test the sensitivity of precipitation by keeping the same temperature record and adjusting precipitation from -20 to 20 % with an increment of 2 %. In addition, we did similar control experiments to explore the sensitivity of temperature and precipitation in different seasons.

2.3 Establishing Regional Chronology and Mapping LIA Glacier

The simulated timing and extent of glacial advances are validated with the ^{10}Be surface exposure ages of the LIA moraines and the mapping of LIA glaciers over BH. Previous studies have dated some well-preserved moraine sequences to represent the time of regional glacial advances during the LIA. Five ^{10}Be ages from moraine M1 of Cogarbu valley and seven ^{10}Be ages from moraine M1 of Shi Mo valley were chosen to determine the regional glaciation chronology establishing in BH (Fig. 1b and Fig. S1). We also chose 126 ^{10}Be surface exposure ages across the monsoonal Himalayas for regional chronological comparison (Table S1). The criteria of ^{10}Be surface exposure ages and moraine ages recalculated are shown in Text S1.

Based on regional glacial chronology and the evidence of sediment-landform assemblages (Chandler et al., 2019), we map the lateral and terminal moraines in BH to represent the maximum extent of glaciers during the LIA. The LIA moraines are usually well-preserved with sharp crests, distributed several hundred meters to a few kilometers away from the termini of modern glaciers, and damming a lake in front of modern glaciers (Zhang et al., 2018b; Qureshi et al., 2021). We use the world imagery ESRI (http://goto.arcgisonline.com/maps/World_Imagery) and Google Earth high-resolution imagery to delineate the outlines of LIA glaciers based on the LIA moraines. We also downloaded their corresponding contemporary glaciers from Randolph Glacier Inventory V6 datasets (RGI; RGI Consortium, 2017). The area and length of contemporary glaciers are provided in RGI datasets. We calculated the area and the length (using the length of the main flowline) of the LIA glaciers in ArcGIS.

3 The pattern of glacier changes during the LIA

We simulated the continuous response of glaciers to climate change in BH during the LIA using OGGM. Large deviations exist among the simulations using the BCC-CSM, CCSM4, and CESM climate datasets in comparison with the observations (Fig. S2). The simulation based on the CESM climate forcing dataset showed the BH was always ice free during the last

https://doi.org/10.5194/tc-2021-352
Preprint. Discussion started: 21 December 2021

millennium due to high temperature, inconsistent with the fact that glaciers still exist in this area even now. For the BCC-CSM and CCSM4 climate datasets, we found an extraordinary rising in temperature after the 1850s, leading to an unreasonably retreat of glaciers so that the modern glacier extent was far less than observations. These three simulations excessively overestimated the amplitude of glacier changes. Thus, we removed these simulations from the discussion and only focused on the pattern of glacier changes during the LIA based on the simulations of the GISS, IPSL, and MPI experiments.

Similar to previous studies (Goosse et al., 2018; Parkes & Goosse, 2020), we used the glacier length to analyze glacier evolution and evaluate the climate model performance. Four substages (glacial advances) are identified in the GISS, IPSL, and MPI experiments (marked as LIA-4 to LIA-1 from old to young). Fig. 2 and Table S3 illustrate their occurrences, and changes in glacier length, area, and volume.

The simulations for the GISS experiment indicate that the most extensive valley and piedmont glaciers occurred during the early LIA (LIA-4), around 1400s. The total glacier length, area, and volume during LIA-4 were 72.9 %, 175.0 %, and 465.7 % larger than the present, respectively. The second most extensive glacial advance occurred during LIA-3 (about 1520s), following by LIA-1 (about 1880s). The smallest glacial advance (LIA-2) occurred about 1700s with the glacier length, area, volume changes of 37.9 %, 127.8 %, and 354.7 %, respectively.

Similar to the GISS experiment, the maximum changes in glacier length (about 97.6 %), area (about 221.9 %), volume (589.7 %) occurred during LIA-4 for the IPSL experiment. However, the occurrence of LIA-4 in the IPSL experiment (1330s) was older than that in the GISS experiment (about 1400s). The second most extensive glacial advance occurred during LIA-2 (about 1710s) for the climate forcing of IPSL dataset, different from the results of the GISS experiment. The minimum glacial advance occurred during LIA-1 (about 1900s) with the glacier length of 56.4 % longer and the glacier area and volume of 128.9 % and 342.2 % larger than the present, respectively.

These four substages (LIA-4 to LIA-1) occurred at about 1270s, 1470s, 1700s, and 1820s in the MPI experiment, respectively. Focused on the glacier length changes, the most extensive glacial advances occurred during LIA-4 with a glacier length of 117.7 % longer than the present, following by LIA-3, LIA-1, and LIA-2 with 76.6 %, 70.9 %, and 61.7 % longer in glacier length than the present, respectively.

https://doi.org/10.5194/tc-2021-352
Preprint. Discussion started: 21 December 2021

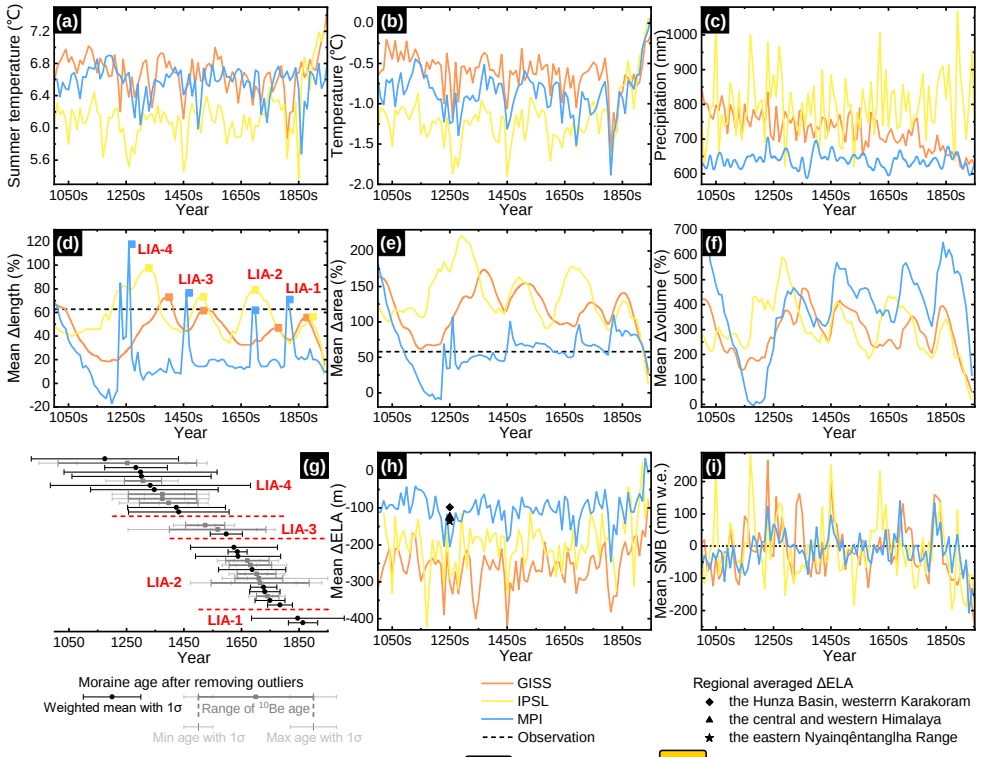

Figure 2. Interannual (a) summer temperature, (b) temperature, and (c) precipitation changes from 1000s to 1950s averaged over Bhutanese Himalaya. Glacier (d) length, (e) area, (f) volume, (h) ELA, and (i) SMB changes during LIA across the studied area, modelled by OGGM using three separate GCM produces (GISS, IPSL, and MPI). Each glacier in the OGGM runs has its length, area, volume, and ELA changes normalized relative to the corresponding averaged parameters during 1950s in the run output. Besides, the recalculated moraine ages across the monsoon-influenced Himalaya are also shown (g). The regional averaged ΔELAs are illustrated in Fig. 2h.

4 Discussions

4.1 The Comparison between Simulations and Observations

We validated the simulation results using mapped LIA glaciers. The regional average length of 408 mapped LIA glaciers is about 62.7 % longer than the present glaciers along the flowlines, similar to the simulation results of the GISS experiment (72.9 %). Simulations with IPSL (97.6 %) and MPI (117.7 %) datasets overestimated the length change of LIA glaciers. A possible explanation for the overestimation of the IPSL and MPI experiments is that the larger amplitude of temperature reduction causes the sharply increasing of positive SMB, leading to the intensively glacier advance during the glacial period.

All of three experiments overestimate the area of LIA glaciers in comparison with the mapped moraines and the studies from nearby area. The mapped total LIA glacier area is about 57.9 % larger than the present value, which is significantly smaller than the simulated 175.0 % for the GISS experiment, 221.9 % for the IPSL experiment, and 109.6 % for the MPI experiment. At the regional scale, the total glacier area has increased about 45.3 % during LIA in the central and western

https://doi.org/10.5194/tc-2021-352
Preprint. Discussion started: 21 December 2021

Himalayas relative to that in 2015 (Qiao & Yi, 2017), and 81.2 % during LIA in the Gangdise Mountains relative to that in 2010 (Zhang et al., 2018b) based on the glacial geomorphological maps. The overestimated of the area change of LIA glaciers is likely caused by two reasons: 1) OGGM is a flowline-based model and the model-derived flowline becomes less valid when glaciers expended to large and complex glaciers (Maussion et al., 2019); and 2) when tributary glaciers merge into a main glacier, OGGM calculates the areas of the tributary and main glaciers repeatedly, overestimating the glacier area (Goosse et al., 2018). The simulated glacier volume further amplified the differences with the overestimated glacier areas as the volume equals to the product of the area and the thickness.

Compared with previous investigations, the model simulates the ΔELA quite well for the MPI experiment but overestimates the ΔELA for GISS and IPSL experiments (Fig. 2h; Loibl et al., 2014; Qiao & Yi, 2017; Qureshi et al., 2021). ELA is the elevation where accumulation equals ablation for a certain glacier (Eq. 1; Benn & Lehmkuhl, 2000; Heyman, 2014). The larger positive SMB makes the glacier advanced and the ELA dropped. Thus, the amplitude of ΔELA is determined by the amplitude of SMB. It seems that the GISS and IPSL climate datasets caused dramatic changes in SMB and higher ELA.

Above all, different climate datasets have different performances for different parameters. The GISS climate dataset performs better for the glacier length change, but the MPI better for the ELA change.

4.2 Why exists four LIA substages in BH?

Although large uncertainties exist in cosmogenic nuclide surface exposure dating, it is still one of main methods to constrain the glacial chronology. Many studies have been conducted in dating the LIA moraines in or nearby our simulation region (Fig. 2g and Table S1). However, the dating results vary with glaciers. For example, only one moraine was dated in Cogarbu valley (1256 ± 56 - 1494 ± 43 CE; Fig. S1; Peng et al., 2019), but two substages were constrained in Lato valley, Lahul Himalaya (Saha et al., 2018), Langtang Khola valley, Nepal Himalaya (Barnard et al., 2006), and Gongotri Ganga valley, Garhwal Himalaya (Barnard et al., 2004). Liu et al. (2017) have found at least three LIA moraines in Lhagoi Kangri Range, Karola Pass. Murari et al. (2014) and Zhang et al. (2018a) have identified at least four LIA moraines in Bhillangana and Dudhganga valleys, Garwal Himalaya, and Lopu Kangri Area, central Gangdise Mountains, respectively. The difference in LIA substages has been explained by the different climate conditions in these areas (Owen & Dortch, 2014; Murari et al., 2014; Saha et al., 2019).

We argue that the difference in LIA substages is caused by the sensitivity of different glaciers rather than the regional climate conditions. We found a negative correlation between the number of LIA substages and the length of glaciers in BH (the correlation coefficients are -0.21, -0.32, and -0.33 for the GISS, IPSL, and MPI experiments, respectively; Fig. 3a and Fig. 3b), indicating that smaller glaciers are more sensitive to climate change compared to larger glaciers (Xu et al., 2011). As illustrated by the frequency of the number of LIA substages of each glacier (Fig. 3b), about 42.1 % of glaciers for the GISS experiment, 60.8 % of glaciers for the IPSL experiment, and 62.0 % of glacier for the MPI experiment have four LIA substages.

https://doi.org/10.5194/tc-2021-352
Preprint. Discussion started: 21 December 2021

Except for the simulation results of the GISS experiment (1364 m), the average length of the glaciers with four LIA substage was about 1628 and 1613 m for the IPSL and MPI experiments, respectively, consistent with the regional average length of modern glaciers (1596 m; Fig. 3a).

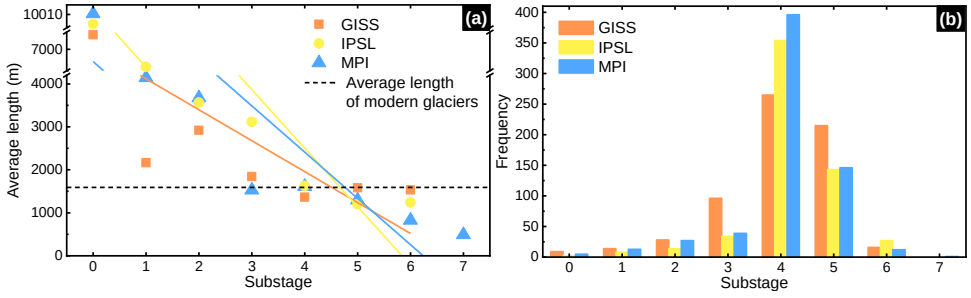

Figure 3. (a) The relationship between the number of substages and the average glacier length of each substage. (b) The frequency distribution chart shows the number of the LIA substages of each glacier.

The number of preserved substages is influenced by the extent of glacial advance in each substage. If the extent of glacial advance is larger during the later substage, the early glacial landforms would be destroyed by glacial advance, causing the lack of earlier substages (Li et al., 2011; Fu et al., 2013). For example, we expect that most moraines will be found during LIA-4, LIA-3, and LIA-1 in the field investigation if the climate follows the GISS and MPI experiments scenario, but lack of the moraines during LIA-2 because of its limited extent of glacier advance than LIA-1. In contrast, most of moraines should be dated to LIA-4, LIA-2, and LIA-1 under the IPSL experiment scenario. Most available ^{10}Be ages concentrated in LIA-4 and LIA-2 (13 and 14 moraines were dated to LIA-4 and LIA-2, respectively; Fig. 2g), indicating that the IPSL experiment captured glacial fluctuations during the LIA (Fig. 2d).

A small number of moraines were dated to LIA-3, such as the moraine m_{bd2} and moraine m_{bk2} in Garhwal Himalaya (Murari et al., 2014) and moraine m_{A2c} in Lato valley (Saha, et al., 2018), indicating that not all glaciers advanced to their second longest length during LIA-2 (the IPSL experiment; Fig. 2d). Our simulations also support this observation. As illustrated in Fig. S4, about 49.0 % of glaciers occurred during LIA-2 and 25.5 % of glaciers occurred during LIA-3. If the dated moraine belongs to these 25.5 % glaciers, the glacier advance would be found. Similarly, not all glaciers advanced to their longest length during the early LIA (LIA-4). For the IPSL experiment, about 98.1 % of glaciers have the longest length during LIA-4, but it is more complex for the simulation results driven by the GISS and MPI climate datasets (Fig. S4). For the MPI experiment, about 80.4 % glaciers advanced most extensive during LIA-4, but there were still about 12.9 % of glaciers have the maximum glacier length change after 1800s (Fig. S5). For the GISS experiment, these two numbers were 47.2 % and 29.3 % (Fig. S3). If we chose the glaciers which reached their most extensive glacial advance after 1800s, the glacial landforms before 1800s would be destroyed.

In summary, the regional glacial evolution is a collective effect of individual glacier changes. Four substages during LIA

https://doi.org/10.5194/tc-2021-352
Preprint. Discussion started: 21 December 2021

228 at the regional scale does not guarantee that each individual glacier has four substages. Instead, it only represents the
229 characteristics of most typical glaciers that accounted for the vast majority of the total glaciers. This can explain why there
230 exists four substages in regional scale in the simulation but is hard captured in the previous studies that only focus on one
231 individual glacier, which helps us to deeply understand the relationship between regional glacial evolution and the individual
232 glacier response to climate change.

233 **4.3 Climate-forcing Mechanisms**

234 Positive or negative SMB determines whether a glacier advances or retreats, and the amplitude of glacier change is
235 directly influenced by the amplitude of SMB change and the duration of the positive or negative SMB (Marzeion et al., 2012;
236 Maussion et al., 2019; Fig. 2i). Previous studies indicated that the change of SMB is determined by the temperature and
237 precipitation change according to the PDD scheme and the climatic proxy comparison (Eq. 1; Fig. 2a-2c; Marzeion et al., 2012;
238 Maussion et al., 2019; Peng et al., 2019, 2020; Parkes, et al., 2020). Our study revealed that the summer temperature plays a
239 dominant role in controlling glacier changes at suborbital-scale.

240 Figure 4 illustrates the average monthly temperature, precipitation and ΔSMB for the GISS, IPSL, and MPI experiments
241 during LIA and at present. For these three experiments, the magnitudes of SMB changes in summer are about 224, 167, and
242 113 mm w.e., accounting for 82.6 %, 71.8 %, and 85.2 % to the annual ΔSMB, respectively, indicating that the summer climate
243 condition dominants the change of annual SMB. Although the increasing summer precipitation are about 70.3, 51.9, and 8.5
244 mm, accounting for 83.9 %, 76.7 %, and 130.2 % for the annual precipitation, precipitation is mainly categorized as liquid in
245 the model due to that the average summer temperature was about 6.6 ℃ during LIA, larger than 2 ℃ (Eq. 1). Thus, glacier
246 accumulation is less during the summer. On the other hand, the summer temperature decreased about -0.9, -1.2, and -0.3 ℃
247 for these three experiments, respectively. The reduced summer temperature decreased the cumulative positive temperature,
248 resulting in the reduction in summer ablation (Eq. 1). The SMB is determined by both the ablation and the accumulation (Peng
249 et al., 2020). Although the accumulation did not change too much in summer, the low summer temperature reduces the ablation,
250 resulting in an increase in the SMB of glaciers.
251

https://doi.org/10.5194/tc-2021-352
Preprint. Discussion started: 21 December 2021

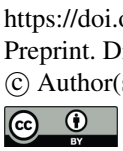

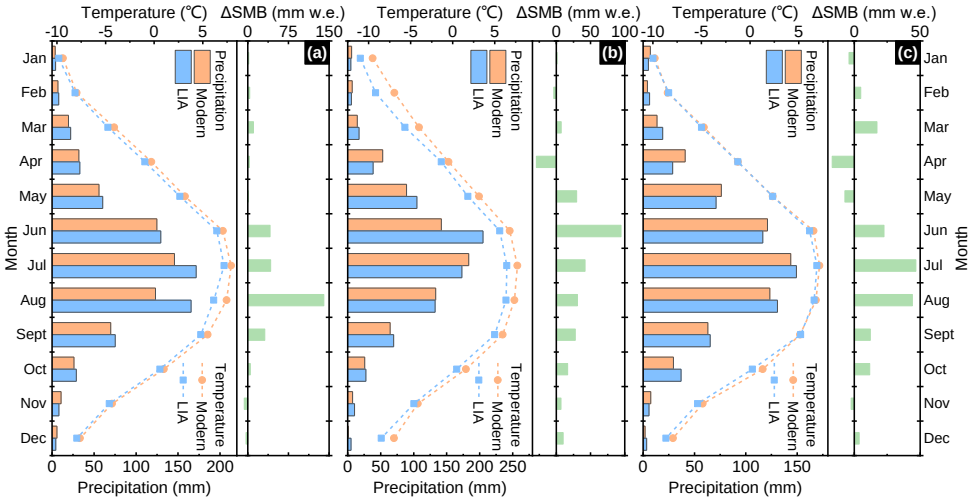

Figure 4. The average monthly temperature, precipitation, and ΔSMB during LIA (from LIA-4 to LIA-1) and modern (1950s) of (a) GISS, (b) IPSL, and (c) MPI.

We also conducted the sensitivity analysis to examine the influence of seasonal temperature or precipitation on glacier change (Fig. 5). Glaciers shrink gradually in response to increasing annual temperature from 0.1 to 0.4 ℃ and disappear after the annual temperature is larger than 0.5 ℃ or after the summer temperature larger than 0.8 ℃. The regional averaged glacier length increases linearly when the annual temperature decreases from 0.1 to 1.0 ℃, with an average rate of 1600 m/℃. Applying the same simulation strategy, the change rates of glacier length due to the temperature decreasing in spring, summer, autumn, and winter are estimated as 82, 1008, 602, and 0 m/℃, respectively, account for 5 %, 63 %, 38 %, and 0 % of the annual change. These results confirm that the temperature changes in summer and autumn seasons explain >90 % variance of the changes in glacier length.

When forced by an increase of present-day annual precipitation of 2 % to 20 % with keeping temperature fixed, the model, predicts an increase of the glacier length by 31 m per % precipitation increase. For seasonal precipitation changes from 102 to 120 % of present-day values, the changes in glacier length are higher in spring (18 m/%) and autumn (12 m/%), followed by winter (5 m/%) and summer (2 m/%). Therefore, the precipitation increases in the spring and autumn have more influences on glacier changes.

Based on the seasonal temperature changes (Fig. 4) for the GISS, IPSL, and MPI experiments and the glacier length change sensitivity to temperature mentioned above, the glacier length increased about 187.1 %, 267.5 %, 91.0 % longer than the present (672 m), respectively. Similarly, the glacier length increased about 35.2 %, 37.2 %, 1.2 % for the GISS, IPSL, and MPI experiments, respectively. Compared with the glacier length change caused by seasonal temperature and precipitation change, we argue that the change in temperature, especially summer temperature, is the dominant forcing factor for glacier changes during the LIA. In contrast, the impact of precipitation change is limited. In addition, the amplitude of glacier length change is larger for the steady-state simulation than that for the continuous simulation because the glacial response to climate

https://doi.org/10.5194/tc-2021-352
Preprint. Discussion started: 21 December 2021

275 change always takes thousands of years, or even longer, during which the climate has become warm.

276

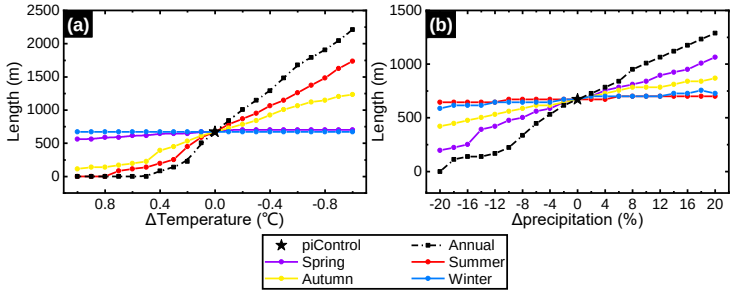

277

278 **Figure 5. Sensitivity of glacier length to annual or seasonal (a) temperature and (b) precipitation perturbations.**

279 **5 Conclusions**

280 We simulated the glacial evolution across BH over the past millennium using the coupled mass-balance and ice flow
281 model, OGGM. Compared with the geomorphological maps and ^{10}Be exposure ages, OGGM broadly captures the amplitude
282 of glacier length changes, especially for the GISS climate datasets. The ELA changes driven by MPI climate dataset are
283 consistent with the regional averaged ΔELA nearby BH, but the model overestimates ΔELA for GISS and IPSL experiments.
284 In addition, OGGM overestimates glacier extent in a factor of >2 due to the limitation of the model.

285 Four LIA substages were identified at about 1270s-1400s, 1470s-1520s, 1700s-1710s, and 1820s-1900s (from LIA-4 to
286 LIA-1) based on the simulations. The IPSL dataset is better to reconstruct the pattern of glacier changes in BH. The most and
287 second extensive glacial advances occurred during LIA-4 and LIA-2 for the IPSL experiment, consistent with regional glacial
288 chronological and geomorphic evidence. The number of the substages for individual glacier has a negative correlation with
289 glacier length, and the amplitude of length change for each glacier is also varying from different features of glaciers. The
290 regional pattern of glacier changes represented the characteristics of most glaciers.

291 The glacier advances are dominated by the reduction of summer ablation. Specifically, glaciers were more sensitive to the
292 changes in the summer and autumn temperature or the spring and autumn precipitation in BH.

293 Although limitations still exist in the simulations, such as the application of OGGM on glacier area and volume changes,
294 this study presented the first simulation of sub-millennium glacial evolutions during LIA in BH using the OGGM. We also
295 found a testable relationship between seasonal climate change and glacier expansion. Our findings provide important insights
296 into the climate forcing mechanism on glacier change at centennial timescale. The evaluation of the effects of different climate
297 datasets on glacier change helps choose the suitable climate dataset for predicting the changes of glacier and water sources in
298 response to future climate change.

299 **Code and data availability.** Code to run OGGM v1.2 is available at https://doi.org/10.5281/zenodo.2580277 (Maussion et
300 al., 2019).

301 **Author contributions.** Study concept devised by CW. YW performed the model runs and analysis, and wrote the original

draft. LY and LG reviewed and revised the paper.

Competing interests. The authors declare that they have no conflicting interests.

Acknowledgments. This work was supported by the Second Tibetan Plateau Scientific Expedition and Research (STEP; grant no. 2019QZKK0205) and the National Natural Science Foundation (NSFC; grant no. 41771005, 41371082).

References

Bahr, D. B., Pfeffer, W. T., and Kaser, G.: A review of volume-area scaling of glaciers. *Rev. Geophys.*, *53*, 95–140, https://doi.org/10.1002/2014RG000470, 2015.

Balco, G., Stone, J.O., Lifton, N.A., and Dunai, T.J.: A complete and easily accessible means of calculating surface exposure ages or erosion rates from ^{10}Be and ^{26}Al measurements, *Quat. Geochronol.*, *3*, 174-195, https://doi.org/10.1016/j.quageo.2007.12.001, 2008.

Barnard, P.L., Owen, L.A., Finkel, R.C., and Asahi, K.: Landscape response to deglaciation in a high relief, monsoon-influenced alpine environment, Langtang Himal, Nepal, *Quaternary. Sci. Rev.*, *25*, 2162-2176, https://doi.org/10.1016/j.quascirev.2006.02.002, 2006.

Barnard, P.L., Owen, L.A., Sharma, M.C., and Finkel, R.C.: Late Quaternary (Holocene) landscape evolution of a monsoon-influenced high Himalayan valley, Gori Ganga, Nanda Devi, NE Garhwal, *Geomorphology*, *61*, 91-110, https://doi.org/10.1016/j.geomorph.2003.12.002, 2004.

Benn, D.I., and Lehmkuhl, F.: Mass balance and equilibrium-line altitudes of glaciers in high-mountain environments, *Quatern. Int.*, *65/66*, 15-29, https://doi.org/10.1016/S1040-6182(99)00034-8, 2000.

Bueler, E., and Brown, J.: Shallow shelf approximation as a "sliding law" in a thermo mechanically coupled ice sheet model, *J. Geophys. Res-Earth.*, *114*, F03008, https://doi.org/10.1029/2008JF001179, 2009.

Carrivick, J.L., Boston, C.M., King, W., James, W.H., Quincey, D.J., Smith, M.W., Grimes, M., and Evans, J.: Accelerated volume loss in glacier ablation zones of NE Greenland, Little Ice Age to present, *Geophys. Res. Lett.*, *46*, 1476–1484, https://doi.org/10.1029/2018GL081383, 2019.

Chandler, B.M.P., Boston, C.M., and Lukas, S.: A spatially-restricted Younger Dryas plateau icefield in the Gaick, Scotland: Reconstruction and palaeoclimatic implications, *Quaternary. Sci. Rev.*, *211*, 107-135, https://doi.org/10.1016/j.quascirev.2019.03.019, 2019.

Dortch, J.M., Owen, L.A., and Caffee, M.W.: Timing and climatic drivers for glaciation across semi-arid western Himalayan-Tibetan orogen, *Quaternary. Sci. Rev.*, *78*, 188-208, http://dx.doi.org/10.1016/j.quascirev.2013.07.025, 2013.

Eis, J., Maussion, F., and Marzeion, B.: Initialization of a global glacier model based on present-day glacier geometry and past climate information: an ensemble approach, *The Cryosphere*, *13*, 3317-3335, https://doi.org/10.5194/tc-13-3317-2019, 2019.

Farinotti, D., Brinkerhoff, D. J., Clarke, G. K. C., Füst, J. J., Frey, H., Gantayat, P., Gillet-Chaulet, F., Girard, C., Huss, M., Leclercq, P. W., Linsbauer, A., Machguth, H., Martin, C., Maussion, F., Morlighem, M., Mosbeux, C., Pandit, A., Portmann,

https://doi.org/10.5194/tc-2021-352
Preprint. Discussion started: 21 December 2021

A., Rabatel, A., Ramsankaran, R., Reerink, T. J., Sanchez, O., Stentoft, P. A., Singh Kumari, S., van Pelt, W. J. J., Anderson, B., Benham, T., Binder, D., Dowdeswell, J. A., Fischer, A., Helfricht, K., Kutuzov, S., Lavrentiev, I., McNabb, R., Gudmundsson, G. H., Li, H., and Andreassen, L. M.: How accurate are estimates of glacier ice thickness? Results from ITMIX, the Ice Thickness Models Intercomparison eXperiment, The Cryosphere, 11, 949–970, https://doi.org/10.5194/tc-11-949-2017, 2017.

Fu, P., Stroeven, A.P., Harbor, J.M., Hättestrand, C., Heyman, J., Caffee, M.W., and Zhou, P.: Paleoglaciation of Shaluli Shan, southeastern Tibetan Plateau, *Quaternary. Sci. Rev.*, *64*, 121-135, http://dx.doi.org/10.1016/j.quascirev.2012.12.009, 2013.

Goosse, H., Barriat, P-Y., Dalaiden, Q., Klein, F., Marzeion, B., Maussion, F., Pelucchi, P., and Vlug, A.: Testing the consistency between changes in simulated climate and Alpine glacier length over the past millennium, *Clim. Past.*, *14*, 1119-1133, https://doi.org/10.5194/cp-14-1119-2018, 2018.

Greve, R.: A continuum-mechanical formulation for shallow polythermal ice sheets. *Philos. T.R. Soc. A.*, *355*(1726), 921-974, https://doi.org/10.1175/1520-0442(1997)010<0901:AOAPTD>2.0.CO;2, 1997a.

Greve, R.: Application of a polythermal three-dimensional ice sheet model to the Greenland ice sheet: Response to steady-state and transient climate scenarios, *J. Climate.*, *10*(5), 901-918, https://doi.org/10.1098/rsta.1997.0050, 1997b.

Grove, J.M.: *Little Ice Age, 2 ed*, Routledge, 2013.

Heyman, J.: Paleoglaciation of the Tibetan Plateau and surrounding mountains based on exposure ages and ELA depression estimates, *Quaternary. Sci. Rev.*, *91*, 30-41, http://dx.doi.org/10.1016/j.quascirev.2014.03.018, 2014.

Heyman, J., Stroeven, A.P., Harbor, J.M., and Caffee, M.W.: Too young or too old: Evaluating cosmogenic exposure dating based on an analysis of compiled boulder exposure ages, *Earth. Planet. Sc. Lett.*, *302*, 71-80, https://doi.org/10.1016/j.epsl.2010.11.040, 2011.

Li, Y., Liu, G., Kong, P., Harbor, J., Chen, Y., and Caffee, M.: Cosmogenic nuclide constraints on glacial chronology in the source area of the Urumqi River, Tian Shan, China, *J. Quaternary. Sci*, *26*(3), 297-304, https://doi.or/10.1002/jqs.1454, 2011.

Lipscomb, W.H., Price, S.F., Hoffman, M.J., Leguy, G.R., Bennett, A.R., Bradley, S.L., Evans, K.J., Fyke, J.G., Kennedy, J.H., Perego, M., Ranken, D.M., Sacks, W.J., Salinger, A.G., Vargo, L.J., and Worley, P.J.: Description and evaluating of the Community Ice Sheet Model (CISM) v2.1, *Geosci. Model. Dev.*, *12*, 387-424, https://doi.org/10.5194/gmd-12-387-2019, 2019.

Loibl, D., Lehmkuhl, F., and Grießinger, J.: Reconstructing glacier retreat since the Little Ice Age in SE Tibet by glacier mapping and equilibrium line altitude calculation, *Geomorphology*, *214*, 22-39, http://dx.doi.org/10.1016/j.geomorph.2014.03.018, 2014.

Liu, J., Yi, C., Li, Y., Bi, W., Zhang, Q., and Hu, G.: Glacial fluctuations around the Karola Pass, eastern Lhagoi Kangri Range, since the Last Glacial Maximum, *J. Quaternary. Sci*, *32*(4), 516-527, https://doi.org/10.1002/jqs.2946, 2017.

Marzeion, B., Jarosch, A. H., and Hofer, M.: Past and future sea-level change from the surface mass balance of glaciers, *The Cryosphere*, *6*, 1295–1322, https://doi.org/10.5194/tc-6-1295-2012, 2012.

https://doi.org/10.5194/tc-2021-352
Preprint. Discussion started: 21 December 2021

366 Maussion, F., Butenko, A., Champollion, N., Dusch, M., Eis, J., Fourteau, K., Gregor, P., Jarosch, A. H., Landmann, J., Oesterle,
367 F., Recinos, B., Rothenpieler, T., Vlug, A., Wild, C. T., and Marzeion, B.: The Open Global Glacier Model (OGGM) v1.1,
368 Geosci. Model Dev., 12, 909–931, https://doi.org/10.5194/gmd-12-909-2019, 2019.
369 Murari, M.K., Owen, L.A., Dortch, J.M., Caffee, M.W., Dietsch, C., Fuchs, M., Haneberg, W.C., Sharma, M.C., and Townsend-
370 Small, A.: Timing and climatic drivers for glaciation across monsoon-influenced regions of the HimalayaneTibetan orogen,
371 *Quaternary Science Review*, *88*, 159-182, http://dx.doi.org/10.1016/j.quascirev.2014.01.013, 2014.
372 Oerlemans, J., Anderson, B., Hubbard, A., Huybrechts, Ph., Jóhannesson, T., Knap, W.H., Schmeits, M., Stroeven, A.P., van
373 de Wal, R.S.W., and Zuo, Z.: Modelling the response of glaciers to climate warming, *Climate Dynamics*, *14*, 267-274,
374 https://doi.org/10.1007/s003820050222, 1998.
375 Owen, L.A.: Latest Pleistocene and Holocene glacier fluctuations in the Himalaya and Tibet, *Quaternary. Sci. Rev.*, *28*, 2150-
376 2164, https://doi.org/10.1016/j.quascirev.2008.10.020, 2009.
377 Owen, L.A., and Dortch, J.M.: Nature and timing of Quaternary glaciation in the Himalayan-Tibetan orogen, *Quaternary. Sci.*
378 *Rev.*, *88*, 14-54, http://dx.doi.org/10.1016/j.quascirev.2013.11.016, 2014.
379 PAGES 2k-PMIP3 group.: Continental-scale temperature variability in PMIP3 simulations and PAGES 2k regional
380 temperature reconstructions over the past millennium, *Clim. Past.*, *11*, 1673-1699, https://doi.org/10.5194/cp-11-1673-2015,
381 2015.
382 Parkes, D., and Goosse, H.: Modelling regional glacier length changes over the last millennium using the Open Global Glacier
383 Model, *The Cryosphere*, *14*, 3135-3153, https://doi.org/10.5194/tc-14-3135-2020, 2020.
384 Pelto, B.M., Maussion, F., Menounos, B., Radić, V and Zeuner, M.: Bias-corrected estimates of glacier thickness in the
385 Columbia River Basin, Canada, *J. Glaciol*, *66*(260), 1051-1063, https://doi.org/10.1017/jog.2020.75, 2020.
386 Peng, X., Chen Y., Liu, G., Liu, B., Li, Y., Liu, Q., Han, Y., Yang, W., and Cui, Z.: Late Quaternary glaciations in the Cogarbu
387 valley, Bhutanese Himalaya, *J. Quaternary. Sci*, *34*(1), 40-50, http://dx.doi.org/10.1002/jqs.3079, 2019.
388 Peng, X., Chen, Y., Li, Y., Liu, B., Liu, Q., Yang, W., Liu, G.: Late Holocene glacier fluctuations in the Bhutanese Himalaya,
389 *Global. Planet. Change.*, *187*, 103137, https://doi.org/10.1016/j.gloplacha.2020.103137, 2020.
390 Qiao, B., and Yi, C.: Reconstruction of Little Ice Age glacier area and equilibrium line attitudes in the central and western
391 Himalaya, *Quatern. Int.*, *444*, 65-75, http://dx.doi.org/10.1016/j.quaint.2016.11.049, 2017.
392 Qureshi, M.A., Li, Y., Yi, C., and Xu, X.: Glacial changes in the Hunza Basin, western Karakoram, since the Little Ice Age,
393 *Palaeogeogr. Palaeocl.*, *562*, 110086, https://doi.org/10.1016/j.palaeo.2020.110086, 2021.
394 RGI Consortium.: Randolph Glacier Inventory (RGI)-A Dataset of Global Glacier Outlines: Version 6.0,
395 https://doi.org/10.7265/N5-RGI-60, 2017.
396 Saha, S., Owen, L.A., Orr, E.N., and Caffee, M.W.: High-frequency Holocene glacier fluctuations in the Himalayan-Tibetan
397 orogen, *Quaternary. Sci. Rev.*, *220*, 372-400, https://doi.org/10.1016/j.quascirev.2019.07.021, 2019.

https://doi.org/10.5194/tc-2021-352
Preprint. Discussion started: 21 December 2021

398 Saha, S., Owen, L.A., Orr, E.N., & Caffee, M.W.: Timing and nature of Holocene glacier advances at the northwestern end of
399 the Himalayan-Tibetan orogen, *Quaternary. Sci. Rev.*, *187*, 177-202, https://doi.org/10.1016/j.quascirev.2018.03.009, 2018.
400 Schmidt, G. A., Jungclaus, J. H., Ammann, C. M., Bard, E., Braconnot, P., Crowley, T. J., Delaygue, G., Joos, F., Krivova,
401 N.A., Muscheler, R., Otto-Bliesner, B.L., Pongratz, J., Shindell, D.T., Solanki, S.K., Steinhilber, F., and Vieira, L.E.A.: Climate
402 forcing reconstructions for use in PMIP simulations of the last millennium (v1.0), *Geosci. Model. Dev.*, *4*, 33-45,
403 https://doi.org/10.5194/gmd-4-33-2011, 2011.
404 Solomina, O.N., Bradley, R.S., Hodgson, D.A., Ivy-Ochs, S., Jomelli, V., Mackintosh, A.N., Nesje, A., Owen, L.A., Wanner,
405 H., Wiles, G.C., and Young, N.E.: Holocene glacier fluctuations, *Quaternary. Sci. Rev.*, *111*, 9-34,
406 http://dx.doi.org/10.1016/j.quascirev.2014.11.018, 2015.
407 Taylor, K., Stouffer, R., and Meehl, G.: An Overview of CMIP5 and the Experiment Design, *B. Am. Meteorol. Soc.*, *93*, 485-
408 498, https://doi.org/10.1175/BAMS-D-11-00094.1, 2012.
409 Winkelmann, R., Martin, M.A., Haseloff, M., Albrecht, T., Bueler, E., Khroulev, C., and Levermann, A.: The Potsdam Parallel
410 Ice Sheet Model (PISM-PIK) – Part 1: Model description, *The Cryosphere*, *5*, 715-726, https://doi.org/10.5194/tc-5-715-2011,
411 2011.
412 Xu, X., Pan, B., Hu, E., Li, Y., and Liang, Y.: Responses of two branches of Glacier No. 1 to climate change from 1993 to
413 2005, Tianshan, China, *Quatern. Int.*, *236*, 143-150, https://doi.org/10.1016/j.quaint.2010.06.013, 2010.
414 Yan, Q., Owen, L. A., Wang, H., and Zhang, Z.: Climate constraints on glaciation over High-Mountain Asia during the last
415 glacial maximum, *Geophys. Res. Lett.*, *45*, 9024–9033, https://doi.org/10.1029/2018GL079168, 2018.
416 Yan, Q., Owen, L. A., Zhang, Z., Wang, H., Wei, T., Jiang, N., and Zhang, R.: Divergent evolution of glaciation across High-
417 Mountain Asia during the last four glacial-interglacial cycles, *Geophys. Res. Lett.*, *48*, e2021GL092411,
418 https://doi.org/10.1029/2021GL092411, 2021.
419 Yan, Q., Owen, L.A., Zhang, Z., Jiang, N., and Zhang, R.: Deciphering the evolution and forcing mechanisms of glaciation
420 over the Himalayan-Tibetan orogen during the past 20,000 years, *Earth. Planet. Sc. Lett.*, *541*, 116295,
421 https://doi.org/10.1016/j.epsl.2020.116295, 2020.
422 Zhang, Q., Yi, C., Dong, G., Fu, P., Wang, N., and Capolongo, D.: Quaternary glaciations in the Lopu Kangri area, central
423 Gangdise Mountains, southern Tibetan Plateau, *Quaternary. Sci. Rev.*, *201*, 470-482,
424 https://doi.org/10.1016/j.quascirev.2018.10.027, 2018a.
425 Zhang, Q., Yi, C., Fu, P., Wu, Y., Liu, J., and Wang, N.: Glacier change in the Gangdise Mountains, southern Tibet, since the
426 Little Ice Age, *Geomorphology*, *306*, 51-63, https://doi.org/10.1016/j.geomorph.2018.01.002, 2018b.